Journal of Molecular Structure 1288 (2023) 135699

Contents lists available at ScienceDirect

Journal of Molecular Structure

journal homepage: www.elsevier.com/locate/molstr

Assessment of shock wave assisted crystallographic structural stability of poly-crystalline and single crystalline lithium sulfate monohydrate crystals

A. Sivakumar [a,*], P. Eniya [b], S. Sahaya Jude Dhas [c], Lidong Dai [a,*], Raju Suresh Kumar [d], Abdulrahman I. Almansour [d], A. Sakthisabarimoorthi [e], J. Kalyana Sundar [b], S.A. Martin Britto Dhas [f,*]

[a] Key Laboratory of High-temperature and High-pressure Study of the Earth's Interior, Institute of Geochemistry, Chinese Academy of Sciences, Guiyang, Guizhou 550081, China
[b] Department of Physics, Periyar University, Salem, Tamil Nadu 636 011, India
[c] Department of Physics, Kings Engineering College, Sriperumbudur, Chennai, Tamilnadu 602 117, India
[d] Department of Chemistry, College of Science, King Saud University, P.O. Box 2455, Riyadh 11451, Saudi Arabia
[e] School of Materials Science and Engineering, Yeungnam University, 38541, South Korea
[f] Shock Wave Research Laboratory, Department of Physics, Sacred Heart College, Abdul Kalam Research Center, Tirupattur, Vellore, Tamil Nadu 635 601, India

ARTICLE INFO

Keywords:
$Li_2SO_4.H_2O$
Shock waves
Lattice disorder
Magnetic properties

ABSTRACT

In the present work, we demonstrate the interesting findings of shock wave recovery experiment conducted on poly-crystalline lithium sulfate monohydrate crystals ($Li_2SO_4.H_2O$) under 50 and 100 shock pulses loaded conditions and the obtained results are compared to the obtained results of single crystal $Li_2SO_4.H_2O$. The poly-crystalline $Li_2SO_4.H_2O$ samples neither undergo any crystallographic phase transitions nor shock wave assisted dehydration. But, the attained diffraction and Raman results indicate that, at shock loaded conditions, lots of structural deformation and distortions occur in the mother crystal structure by the impact of shock waves. Also, at shocked conditions, the super-paramagnetic state of $Li_2SO_4.H_2O$ is significantly affected and remarkable reduction (10^{-1} to 10^{-7}) of the saturation magnetization is found. Note that, in the case of single crystalline $Li_2SO_4.H_2O$, the disordered crystal structure has been witnessed for shock loaded samples.

1. Introduction

Over a century, consistent progress has been witnessed in materials science research wherein the solid-state phase transitions in materials of ionic sulfate group with respect to pressure and temperature remains to be one of the vibrant research areas such that these group of materials remain to be the most studied to date under static high-temperature as well as high-pressure conditions and several interesting results of crystallographic phase –transitions have been found [1–5]. Note that the polymorphic single crystal of β-K_2SO_4 undergoes the phase transition of α-K_2SO_4 at 851 K due to the rotational disorder of SO_4 units [6]. Na_2SO_4 (phase-V) is converted to the lower symmetry phases such as phase-III and phase-I between 490 and 520 K [7]. Similar to that of K_2SO_4, Li_2SO_4 single crystal also undergoes the phase transition from β *to* α at 848 K [8] whereas in the case of the static pressure compression, the phase of β- Li_2SO_4 is retained up to 13 kbar [9]. $MgSO4{\cdot}7H_2O$ is converted to a lower hydrated crystal structure and finally, the un-hydrated $MgSO_4$ is observed at 573 K [10] and similar results are found for $CuSO_4{\cdot}5H_2O$ [11] as well as $Li_2SO_4.H_2O$ single crystal [12] while subjected to high-temperature. On analyzing various existing results of static high-temperature and pressure effects on solid state sulfate anionic materials, results on phase transitions of the sulfate anionic crystals at dynamic shock wave exposure conditions is relatively a new area of research in materials science branch. On the other hand, it has been witnessed several spectacular results of structural phase transition at shock loaded conditions as in the case of crystals such as K_2SO_4, Na_2SO_4, Li_2SO_4, $MgSO_4{\cdot}7H_2O$, $CuSO_4{\cdot}5H_2O$ and $Li_2SO_4.H_2O$ [13–18].

Moreover, the respective single crystals have been subjected to shock loading and found some interesting results in their crystallographic features. Note that, in the case of K_2SO_4 crystal, the transition of β-K_2SO_4 to α-K_2SO_4 has been observed at one shock pulse exposed condition and α-K_2SO_4 reverts to β-K_2SO_4 at two shock pulses exposed condition [13]. Similar kind of reversible phase transition of phase-V to phase-III has been achieved for Na_2SO_4 single crystal at shock pulses loaded

* Corresponding authors.
E-mail addresses: sivakumar@mail.gyig.ac.cn (A. Sivakumar), dailidong@vip.gyig.ac.cn (L. Dai), martinbritto@shctpt.edu (S.A.M.B. Dhas).

https://doi.org/10.1016/j.molstruc.2023.135699
Received 28 February 2023; Received in revised form 18 April 2023; Accepted 1 May 2023
Available online 9 May 2023

conditions [14]. During the shock pulses loaded conditions, the mixed phase formation of $MgSO_4{\cdot}7H_2O$ and $MgSO_4.6H_2O$ is noticed in the case of the $MgSO_4.7H_2O$ [16]. More interestingly, in the case of $CuSO_4{\cdot}5H_2O$ and $Li_2SO_4.H_2O$ single crystals, disordered crystalline states have been observed at dynamic shock loaded conditions and on further increasing the number of shock pulses, disordered structures have been converted into highly ordered structures [17,18]. On continuing with the same experiment provided with higher number of shock pulses such as 50 and 100, the powder samples of K_2SO_4, Na_2SO_4 and $CuSO_4{\cdot}5H_2O$ have been studied such that there is no crystallographic change found even at 100 shock pulses exposed conditions [19–21]. It is found to be quite an interesting result while compared to the single crystals of those materials and such kind of comparative analysis of single and poly-crystalline structural stability at dynamic shock loaded conditions can lead to a better understating on the shock resistance of solid state materials which leads to acquire knowledge of the materials properties and their functions in extreme conditions.

Along these lines, in this framework, the authors aim to examine the phase transition probability of poly-crystalline lithium sulfate monohydrate at dynamic shocked conditions. Note that the title sample is an interesting material for the applications point of view and it is a classical material for understanding of dehydration while subjected to high-temperature and pressure. Several researchers have made spectacular publications on the crystal growth of $Li_2SO_4.H_2O$ [22–25] and their functional properties employing various methods [26,27] which includes de-hydration concepts with respect to temperature [28–30]. As per the standard thermo-dynamical point of literature survey on $Li_2SO_4.H_2O$, at 80 °C the water molecule escapes from the crystal lattice so that it is converted into Li_2SO_4 [28–30] and similar kind of dehydration process is expected while at higher number of shock pulses exposed conditions. Furthermore, such kind of new mechanistic and kinetic experiments of dehydrations occurring on crystalline hydrates have provided new directions for the experimental and theoretical researchers to make better convincing solid-state nucleation reactions. Moreover, the water molecule promotes the re-crystallization interface and initiates the progression of new chemical change. In addition to that, the chemical units of the title sample such as Li, SO_4, and H_2O are highly sensitive for the positional disorder, rotational disorder and orientational disorder for the exposed shock pressure and temperature and hence significant changes can occur.

In the present study, the authors demonstrate the crystallographic phase stability and magnetic state stability of the powder sample of $Li_2SO_4.H_2O$ at dynamic shock pulses exposed conditions and the occurrence of the significant lattice deformations and loss of magnetic state at shocked conditions are elaborated. The interesting results of the crystallographic and magnetic state features of the title sample will be discussed in the upcoming sections.

2. Experimental section

The crystal growth of the title material and shock wave loading procedures have been discussed in our previous paper [18] as well as the supplementary section also contains the details. Briefly; The title compound of ($Li_2SO_4.H_2O$) (99% purity) was purchased from the Sigma-Aldrich and the required crystal was grown by employing the conventional slow evaporation technique. 50 ml of deionized water was taken in a beaker and lithium sulfate monohydrate compound was added slowly till the saturation was obtained whereby it was allowed to crystal growth and after 30 days, we have harvested optically transparent crystals. The grown single crystals have been finely grounded and the fine powder has been utilized for the required experimental analyses. In the present case, the required shock waves have been generated by an indigenously developed semi-automatic Reddy Tube (Fig. 1) which has three sections known to be the driver, driven and diaphragm sections that are made of stainless steel. The driver and driven sections consist of long tubes of length 48 cm and 180 cm, respectively while both have an identical inner diameter of 13 mm. Atmospheric air has been used as the input source for the required shock wave generation. When the atmospheric air is compressed into the driver section, at the critical pressure, the diaphragm is ruptured and the shock wave is generated and moves along the driven section. The samples have been placed in the sample holder which is 1 cm away from the end section of the driven tube and when the shock tube propagates the shock wave into the driven section it is launched on the test sample which is placed in the sample holder. For this experiment, a total of four samples have been taken in equal measure while one sample has been kept as the control and the remaining three samples have been used for the shock wave loading. Then, the powder sample has been packed in a pouch which was specially made using the shock window materials possessing an area of 1×1 cm^2 and kept in the sample holder such that the shock wave has been loaded on it. In the present experiment, shock waves of Mach number 2.2 have been utilized possessing the reflected shock transient pressure (P_5) of 2 MPa and temperature (T_5) 864 K. The shock waves from the driven section go on striking the sample which is located 1 cm away from the open end of the driven section. Subsequently, 50, 100 and 150 numbers of shock pulses have been loaded on three different title samples. Note that, while compared to the previous single crystal study [18], the transient pressure (1.0 MPa) has been kept two times higher and the numbers of pulses has been enhanced to 50 and 100 so as to understand better the structural and magnetic state features under shock wave exposed conditions.

3. Analytical characterization details

The analytical instruments details are as follows; Powder X-ray diffraction (PXRD) [Rigaku - SmartLab X-Ray Diffractometer, Japan-$CuK\alpha_1$ as the X-ray source ($\lambda = 1.5407$ Å), with the step precision of ±

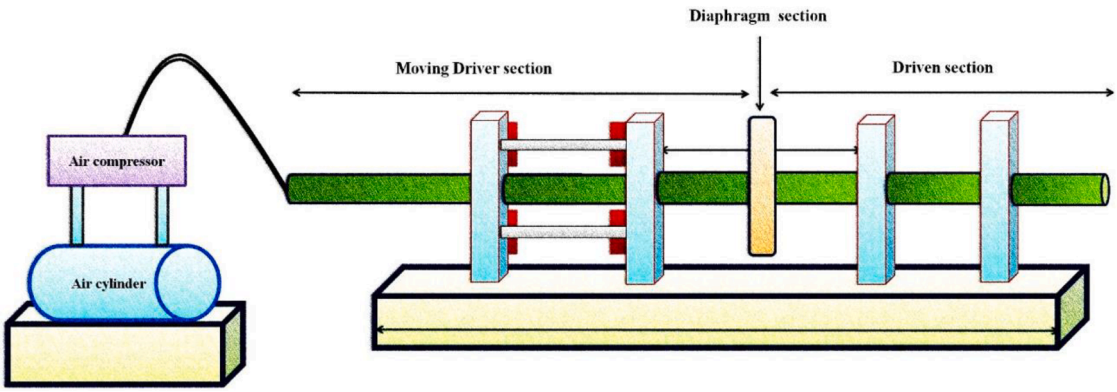

Fig. 1. Schematic diagram of the shock wave loading setup.

0.001°], a Renishaw model Raman spectrometer with Laser line 532 nm and power 50 mW and the Raman measurement was carried out using the pelletized form of samples. The laser spot size was 50 μm^2 and the optical microscope's objective lens was used such that an X50 long working distance objective lens (WD = 10.6 mm) was utilized and the value of numerical aperture was 0.5 while the Raman data was collected by Renishaw Wire 5.1 instrument control and the data acquisition software. An ultra-violet diffused reflectance spectroscope (UV-DRS-ShimadzuUV-3600 plus) and a vibrating sample magnetometer (Lake Shore, Cryotronics) have been utilized so as to understand the structural and magnetic structural stability of the test samples under shocked conditions.

4. Results and discussion

4.1. Powder XRD analysis

Fig. 2a and b show the respective powder XRD patterns of the poly-crystalline and single crystalline lithium sulfate monohydrate for the control and shock wave exposed samples. As seen in Fig. 2a, the XRD pattern of the control sample is found to be well-matched with the literature [24] which confirms that the sample has crystallized in the $P2_1$ space group and the attained sharp diffraction peaks reflect the good crystalline nature of test sample. In addition to that, based on the control sample's XRD pattern, it has maximum diffraction lines in the region of higher diffraction angle and such higher diffraction lines are highly susceptible for the external parameters such as temperature and pressure. In addition to that, such kind of the higher angle diffraction lines can easily undergo orientational disorder, plane re-orientation and so on at shocked conditions compared to that of the lower angle diffraction lines. These kinds of interesting changes have been explored to a certain extent at shocked conditions [13–21]. Furthermore, the diffraction patterns of the pristine and shock loaded samples are provided in Fig. 2a itself and while looking at the patterns, there is no visible signature for any crystallographic phase transitions that typically observed due to the impact of shock waves as in the case of single crystalline lithium sulfate monohydrate for which the corresponding XRD profiles are shown in Fig. 2b.

Note that, in the case of single-crystalline lithium sulfate mono-hydrate, the $P2_1$ crystal structure undergoes a distorted state due to the impact of 3 counts of shocks possessing the Mach number 1.7 and the transient pressure 1 MPa. But, in the present case, even though 100 shock pulses of 2.0 MPa transient pressure have been loaded, no remarkable structural change is observed in the poly-crystalline samples which have higher structural stability than that of the single crystalline samples at dynamic shock loaded sample [19]. On the other hand, the hydrated lithium sulfate sample should have undergone dehydration since the shock pulses have a high transient temperature (864 K). But, based on the observed XRD results, there is no formation of un-hydrated lithium sulfate at shocked conditions. Moreover, in the case of solid samples, shock wave propagation velocity is very high such that its period of existence is within a few microseconds, and hence the water molecule doesn't get the required time to come out of the test sample's crystal structure, whereas the angle of the water molecular bonds and positions in the unit cell may undergo the possible changes at shocked conditions [16,18,31]. In addition to that, the water molecule is directly connected to the Li tetrahedrons so that SO_4 tetrahedrons and the SO_4 units are highly sensitive to transient pressure and temperature associated with the shock wave [17]. Even though the poly-crystalline lithium sulfate monohydrate samples exhibit a stable crystal structure, subtle internal structural changes, as well as deviations in the degree of crystallinity of the samples, may appear and such details are to be discussed. For a better understanding of the internal structural modifications of the test samples, the magnified forms of the XRD patterns are provided in Fig. 3. The control sample shows the diffraction lines such as (100), (10–1) and (011) which are almost similar to the XRD patterns of the sample at the 50 shocked conditions whereas at the 100 shock pulses exposed conditions, remarkable diffraction peak splitting has occurred such that significant changes have been marked in red circles and such changes appear due to defects and micro-distortions developed in the test crystal structure as well as rotational disorder of the SO_4 units [18] and similar kind of the changes have been noted in the hydrogen-bonded crystalline materials such as potassium dihydrogen phosphate [32] and glycine phosphite [33].

As it is in Fig. 3a, Fig. 3b also exhibits similar results in such a way that the diffraction lines such as (002) (101) and (110) have experienced similar types of diffraction peak splitting at the 100 shock waves exposed condition. During the shocked conditions, the SO_4 site symmetry might have been slightly altered and such changes can be incorporated with the Raman spectral results that are to be elaborated. Furthermore, in Fig. 3c and d, some of the diffraction line intensity and sharpness are observed to have increased while the number of shock pulses are increased and such changes are clearly reflected in the (20–1), (300) and (10–3) planes and such interesting results are due to the shock wave induced dynamic re-crystallization. Alike kind of formation of a high-intensity diffraction line has been obtained in the sample of poly-crystalline copper sulfate pentahydrate at shocked conditions [21]. From the above-discussed notable changes in the crystalline features of the test samples, it is clear that the crystallinity has considerably reduced against the number of shock pulses and such changes may initiate significant changes in optical and magnetic properties.

In Fig. 4, the shock phase profile of the single and poly-crystalline

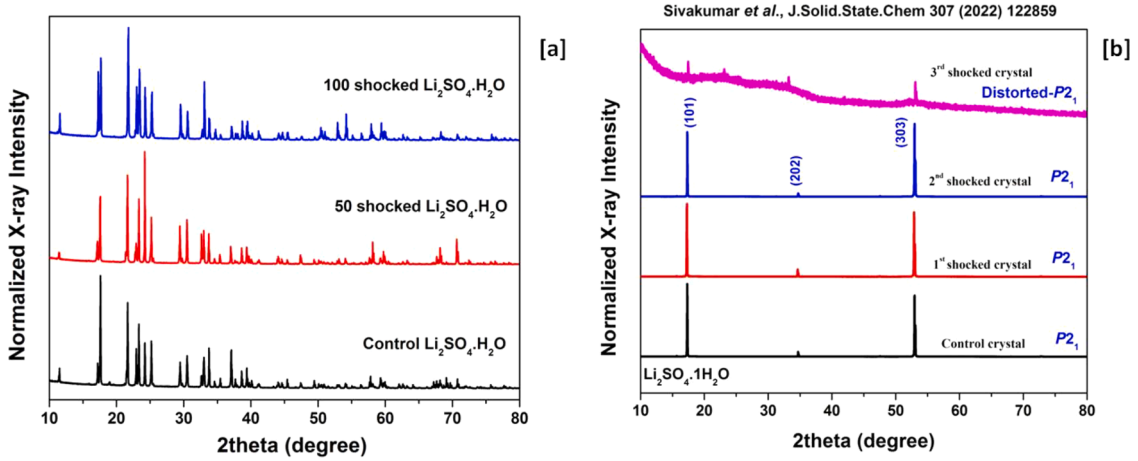

Fig. 2. XRD patterns of (a) the pristine and shock loaded polycrystalline lithium sulfate monohydrate (b) single crystalline lithium sulfate monohydrate [18].

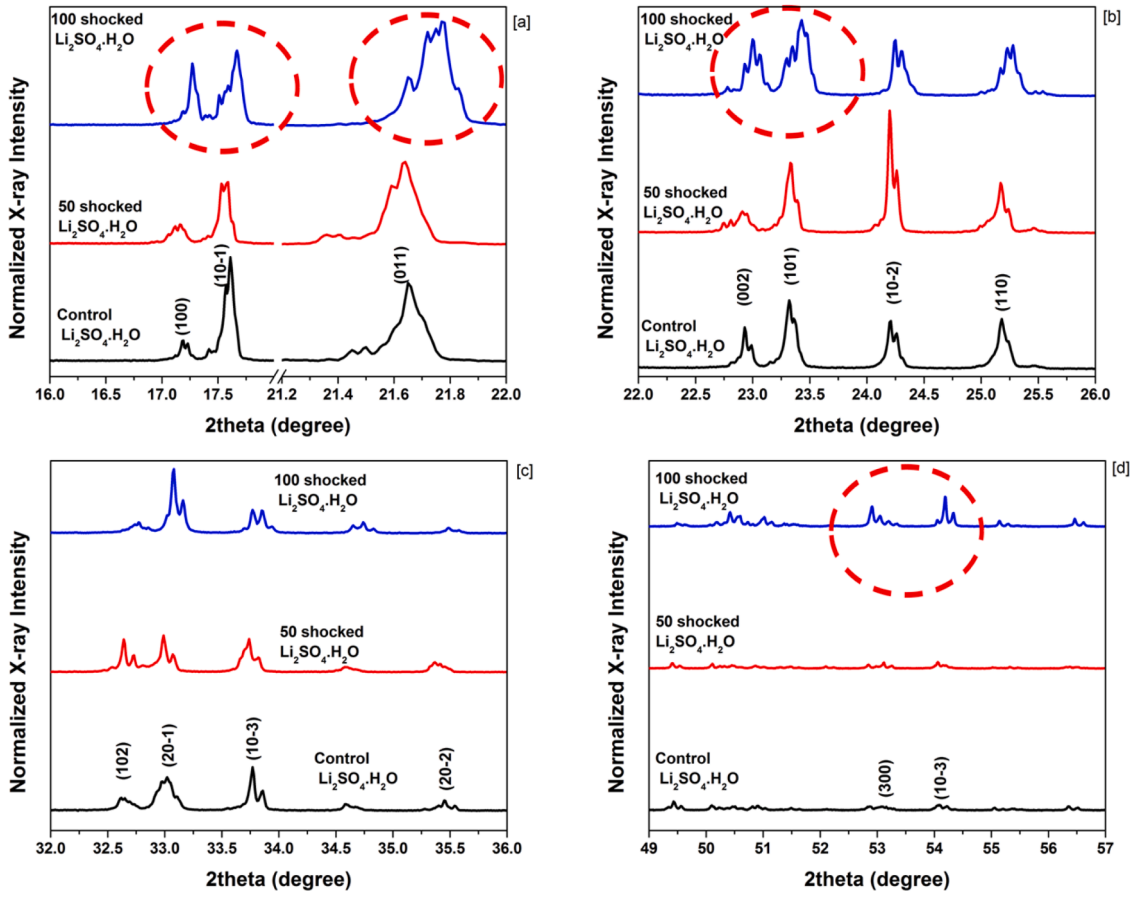

Fig. 3. Magnified version of the XRD patterns of the pristine and shocked samples (a) 16–22° (b) 22–26° (c) 32–36° (d) 49 – 57° .

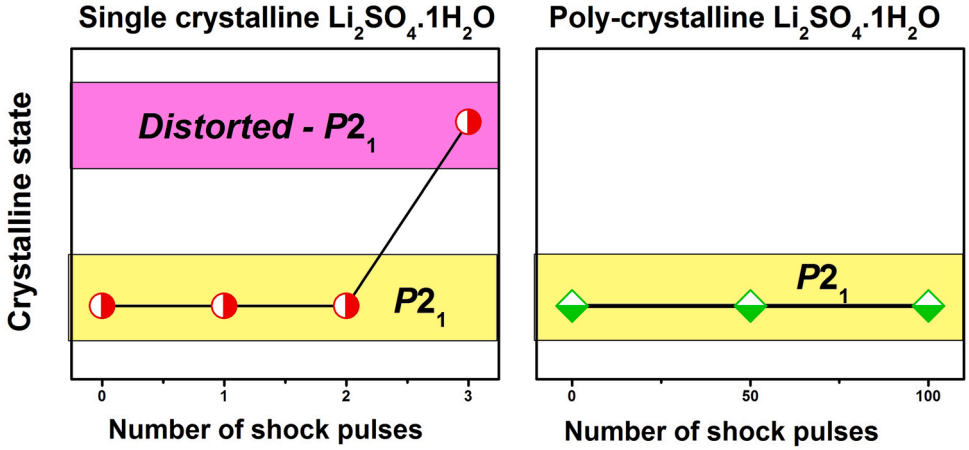

Fig. 4. Shock phase profile of the single and poly-crystalline lithium sulfate monohydrate.

lithium sulfate monohydrate samples is presented and based on the observed profiles, the single-crystalline lithium sulfate monohydrate has very less structural stability than that of the polycrystalline state lithium sulfate monohydrate. The single crystal lithium sulfate monohydrate undergoes the distorted-$P2_1$ space group just at the 3rd shock pulses loaded conditions, but in the case of powder samples, the $P2_1$ space group is retained even at 100 shocked conditions. The possible reasons for such high shock resistance for the poly-crystalline samples are (i) the shock wave propagation in the poly-crystalline samples is highly restrictive due to the high density of the internal grain boundaries [34–36] (ii) the probability of the energy dissipation and scattering of the shock wave is more when passes through the poly-crystalline samples as compared to the single crystal due to a large number of grains so that the net impact of the shock waves is reduced while propagating through the poly-crystalline samples [17,21].

5. Raman spectroscopic results

According to the literature of SO_4 anionic materials at static pressure/temperature [6–12] and shock wave loaded conditions [13–21], the characteristic Raman bands of sulfate ions such as υ_1, υ_2, υ_3, and υ_4 show a few significant modifications based on their internal structural

symmetry and hence Raman spectroscopy has its own importance to justify the structural states and their stabilities of materials while subjecting to the external parameters. The Raman spectral analysis has been performed for the pristine and the shock loaded samples and the observed Raman spectra are displayed in Fig. 5. The control sample has reflected its characteristic Raman bands of sulfate ions i.e. υ_1, υ_2, υ_3, and υ_4 are well corroborated with the literature [37].

From Fig. 5, it is clear that all the characteristic Raman bands of sulfate ions such as υ_1, υ_2, υ_3, and υ_4 are reproduced with the same Raman locations for the pristine and shock wave loaded samples which represent that the sample does not undergo any kind of change in the crystal structure. Note that, if the test sample has undergone the dehydration process, the water molecule would have been ejected from the host crystal structure forming the un-hydrated Li_2SO_4 which belongs to the $P2_1/a$ space group and it should have the doublet degenerate Raman bands of the SO_4 i.e., υ_2, and υ_4 [38,39]. But, surprisingly, such Raman band splitting of singlet to doublet could not be seen at the exposure of shocks which is one of the most crucial justifications for the test sample retaining its own crystal structure. But, while looking at the Raman spectra, the Raman line width, as well as the value of full-width at half maximum, has sufficiently increased against the of shock pulses which reflects the formation of lattice defects. The obtained results of X-ray diffraction also agree well with this claim. The Raman band intensity of υ_2, and υ_3 is sufficiently reduced which indicates the formation of the structural defects, structural distortions and angular changing of the SO_4 tetrahedron [5–12]. In addition to that, υ_3 Raman band undergoes a few Raman band splitting along with the reduction of the original intensity due to the crystal field splitting and symmetry losses of the SO_4 units. Note that, in the case of the single-crystalline lithium sulfate monohydrate, the Raman peak splitting is observed at 3rd shocked conditions due to the formation of the distorted crystal structure of $P2_1$ [18]. From the general spectroscopic point of view, the conversion of a higher Raman band intensity to lower Raman band intensity indicates the reduction of crystalline symmetry in the lattice while several high-pressure compression experimental results carry the similar results for the organic and inorganic materials [40–42]. For example, in the case of Graphite, while increasing the pressure, the characteristic peak of G-band is reduced with respect to pressure which indicates that the perfect graphite is converted into disordered Graphite [42] and similar kind of results have been found in $CaCO_3$ and Oxalyl Dihydrazide under pressure [40,41].

6. Optical properties (DRS spectroscopy)

Fig. 6 portrays the optical transmittance spectra of the pristine and shock loaded samples which are measured by the diffused reflectance spectroscopy. Based on the obtained transmittance spectra; sufficient changes have occurred that could be seen at shocked conditions in terms of the percentage of the optical transmittance spectra. Note that, in the case of the single crystal, significant changes have been found in shock wave exposed samples while in the case of the polycrystalline samples, moderate changes are only observed.

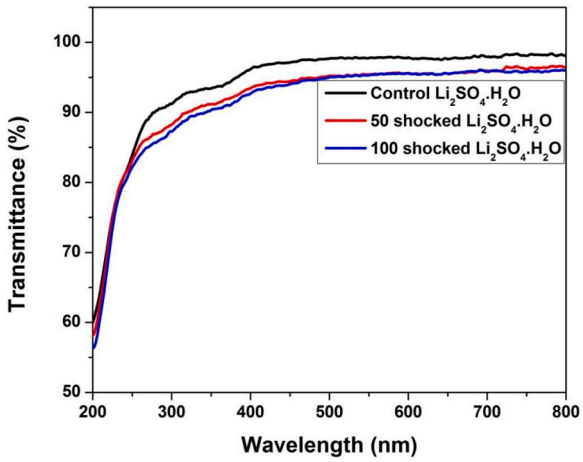

Fig. 6. Optical transmittance spectra of the pristine and shock loaded Li_2SO_4. H_2O powder samples.

For example, in ammonium dihydrogen phosphate single crystal, huge changes are found in the transmittance spectra against the number of shock pulses [43], but slight changes are only observed for the polycrystalline ammonium dihydrogen phosphate [44] and similar kind of results have been witnessed for potassium dihydrogen phosphate samples [32]. Moreover, Dileep et al., have examined the stability in the optical transmittance percentage of lithium sulfate monohydrate against the gamma irradiation (Co-60- 10 kGy, 30 kGy and 50 kGy) and found that the loss of transmittance is due to the generation of surface defects and structural disorder [45]. In this investigation also, a similar type of reduction in the optical transmittance is observed as against the shock pulses (Fig. 7). As seen in Fig. 7, the initial percentage of optical transmittance is 96.3% which is reduced to 93.6% at 50 shocks exposed conditions and further reduced to 92.7% at 100 shocks exposed conditions.

Based on the results of diffraction and Raman spectroscopy obtained in the previous as well as the present experiments, it could be considered that the reduction of the optical transmittance of the test samples at

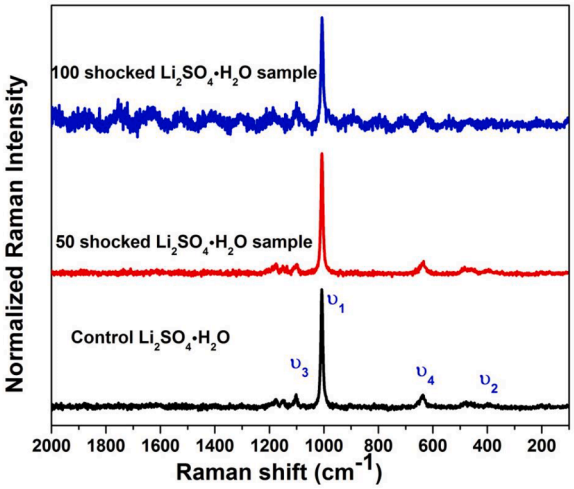

Fig. 5. Raman bands of the pristine and shock wave exposed samples.

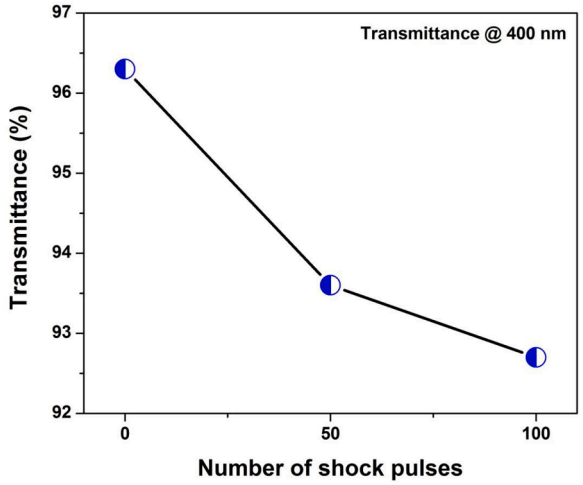

Fig. 7. Optical transmittance against the number of shock pulses.

shocked conditions is due to the formation of the structural defects as well as structural distortions [45]. Note that, in the case of structural phase transitions, massive shifts in absorption band position have been observed in K_2SO_4 crystal [13] and the disappearance of secondary absorption peak has been witnessed for Na_2SO_4 crystal at shocked conditions [14]. Such changes clearly represent that changes occur in the electronic spectra of the test samples at shock conditions. But, in the present case, any such significant electronic spectral changes could not be found rather than a reduction in the optical transmittance spectra of the test samples against the impact of shock waves. Hence, it could be established that the test sample has a stable electronic structure against shock pulses.

7. Magnetic properties

The magnetic response of the solid-state materials is highly sensitive to the order and disorder arrangements of the local atomic structures wherein even a very slight amount of atomic deformations and grain density changes can lead to significant changes in the magnetic state and saturation magnetization [46]. In the present case, the obtained XRD patterns reveal that there is no crystallographic structural transition occurred under shocked conditions. Moreover, structural deformations of the samples could not be witnessed. Hence, there is a possibility of magnetic properties getting greatly alerted such that tremendous differences can happen under shocked conditions. Moreover, the investigation has been extended to acquire a more understanding of the structural dynamics of the test samples under shock wave exposed conditions. The magnetic study of the pristine and shock wave exposed samples has been performed using a vibrating sample magnetometer and the magnetic hysteresis loops are displayed in Fig. 8. The control sample shows the weak ferromagnetic state with the saturation magnetization of 0.1256 emu/g and the obtained results are found to be well-matched with the previous results of lithium-based materials [47, 48]. Surprisingly, for the shock-loaded samples, significant changes can be found in the shape of the hysteresis loop and the complete disappearance of the weak ferromagnetic state of the test samples. A massive reduction of saturation magnetization of the order of 10^{-7} emu/g is witnessed both at 50 and 100 shock pulses exposed conditions. The attained magnetic loops also clearly represent the occurrence of the structural defects as well as changes in the crystal field splitting energy and symmetry losses in the test sample at shocked conditions. Generally, the crystalline materials of higher degrees have the higher saturation magnetization due to the highly ordered magnetic domains and such magnetic domains may collapse at the sudden exposure of shock waves due to the formation of the defects which are typically altered by the spinning state of the materials as well as the crystal field energy profile

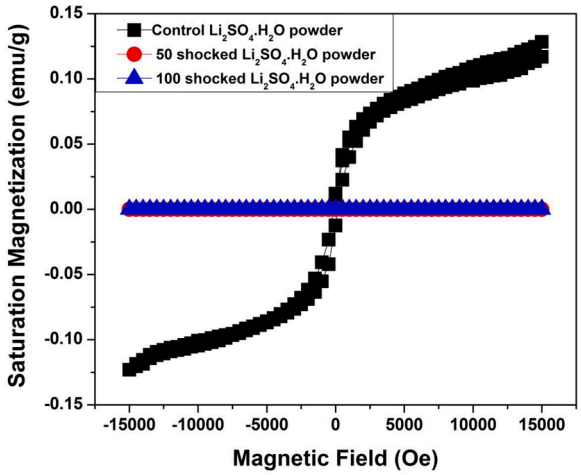

Fig. 8. Magnetic hysteresis loops of the pristine and shock loaded samples.

of the materials [49,50]. In the present case, the sulfate anions may play a vital role in the reduction of magnetic properties under shocked conditions. Because, in the case of lithium sulfate, the compressibility of the anions is significantly lower (14 times) than that of the Li cations and hence the SO_4 tetrahedron may undergo significant rotational disorder which leads to the collapse of the magnetic ordering whereby the lower values of saturation magnetization could be witnessed [18]. At this stage, it is strongly expected that the title crystal might have undergone from usual geometry (Lithium as well as SO_4 units have the tetrahedral geometry) to unusual geometry which significantly alters the orbital splitting thereby resulting in a change in the local magnetic ordering. In this case, the control sample has the perfect tetrahedral geometry which may be lost under shocked conditions [51] due to the higher possibility of the rotational order-disorder process of SO_4 units such that it breaks the long range magnetic ordering which generally leads to the reduction of saturation magnetization [18,46]. In addition to that, reduction of particle size, fragmentation of particles and surface damages have also contributed to the changes in magnetic property which could be analyzed better with the features of SEM image in the next section. Note that similar kinds of results have been observed for the magnetic materials [49,50]. For example, cubic structure Cobalt ferrite nano-crystalline materials have been subjected to the shock waves of counts 0, 50, 100 and 150 shock pulses, respectively wherein at 150 shocked conditions, significant lattice distortions have been noticed and as a result, the values of saturation magnetization are significantly reduced such that the values are found to be 76.5, 77, 75.8 and 40 emu/g, respectively [50]. Moreover, here also similar lattice distortions are expected in the title sample to play a major role in influencing changes in the saturation magnetization under shocked conditions [50] and chemical doping conditions [52].

Based on the obtained magnetic properties against the number of shock pulses, the magnetic structure has undergone significant changes as compared to the crystal structure of the test sample. Note that such kind of remarkable loss of the magnetic state of the test sample at shock loaded conditions may be the first report, to date, for the literature wherein the magnetic state phase transitions occurring at shock wave exposed conditions are well witnessed.

8. Scanning electronic microscopic images

Scanning Electron Microscopic study has been performed to understand the surface morphological characteristics of the control and shocked samples such that the recorded images are presented in Fig. 9. Usually, good crystalline materials have a defect-less surface and vice versa for disordered samples. As seen in Fig. 9a, the control sample has a smooth surface whereon bulk size particles are present in the order of 5–10 μm. On the other hand, under shocked conditions, lots of small particles could be seen in the SEM images captured for the 50 and 100 shocked conditions which clearly disclose the fragmentation of the particles under shocked conditions which may lead to the reduction of particle sizes as well as loss of long-range magnetic ordering. Based on the SEM results, it is quite clear that the sample's mechanical stability is less and due to which the large-size particles may break into two or more parts. In consolidating the observed results, a similar kind of large collapse in the size of the particles has been witnessed for the shock wave-induced amorphous state of ZIF-8 [53,54].

9. Conclusion

We have systematically examined the impact of shock waves on the structural, optical and magnetic behavior of the hydrated form of lithium sulfate under shocked conditions and drawn the conclusion based on the obtained results of XRD, Raman, VSM and SEM techniques. X-ray diffraction and Raman spectral results show that the test sample retains its original structure even at 100 shock loaded conditions, but a few structural distortions and defects are found in the host crystal

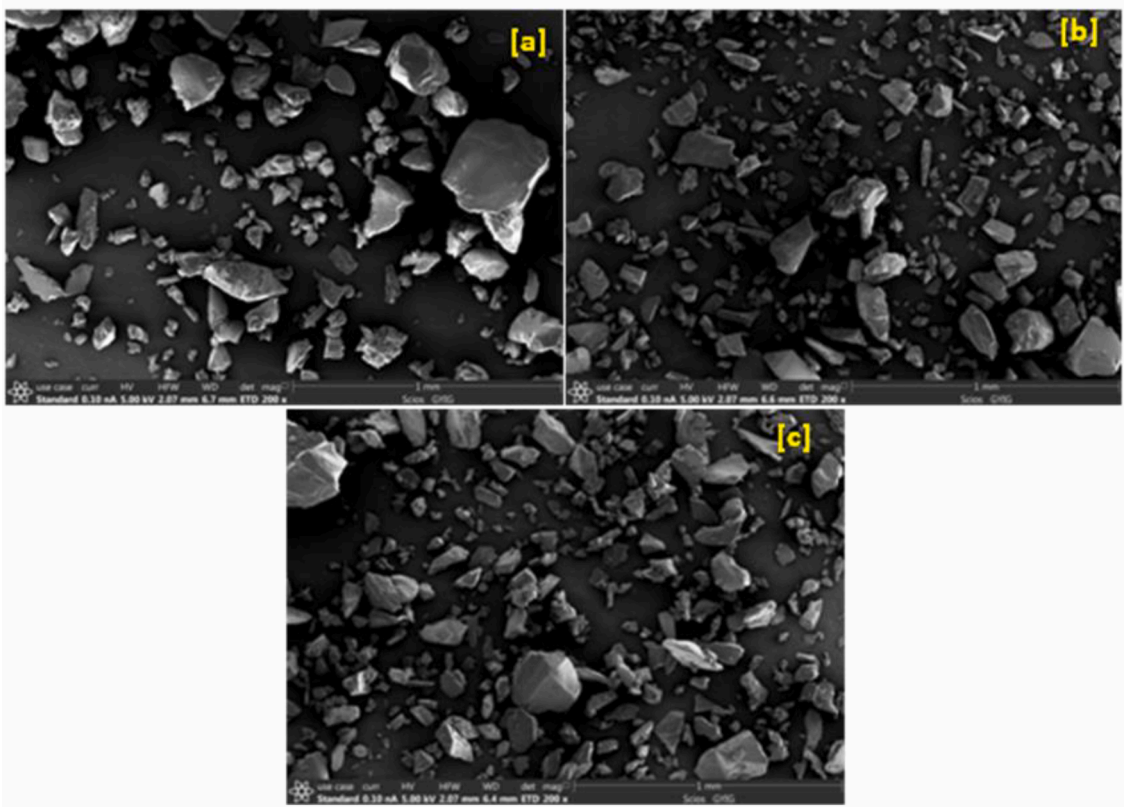

Fig. 9. SEM images of the control and shocked samples (a) 0-shock (b) 50 shocks (c) 100 shocks.

structure because of the formation of shoulder diffraction peaks and Raman band splitting at 100 shocked conditions. The reduction of the Raman spectral intensity provides yet another reasonable evidence for the formation of distorted crystal structure under shocked conditions. Furthermore, considering the optical properties as well as magnetic properties, loss of optical transmittance and massive loss of the saturation magnetization have been found at shock wave exposed conditions. SEM results show the fragmentation of particles under shocked conditions. Hence, from the explored investigations, it could be declared on solid grounds that the crystallographic phase and magnetic phase of the titled polycrystalline sample are less stable against the shock waves. On the other hand, while compared with the single crystals, polycrystalline samples have quite high shock resistance. It is expected that such basic applied research on simple hydrated and un-hydrated materials under shocked conditions could offer yet another way to understand better the structural dynamics of the materials because the sulfate anionic materials are usually used as the traditional materials in exploring the structural phase transitions of solids.

Data availability

Data sharing, evidence of data sharing, and peer review of data are required. The data that support the findings of this study are available from the corresponding author upon reasonable request.

CRediT authorship contribution statement

A. Sivakumar: Data curation, Writing – original draft. **P. Eniya:** Resources. **S. Sahaya Jude Dhas:** Visualization, Writing – original draft. **Lidong Dai:** Supervision, Writing – review & editing. **Raju Suresh Kumar:** Formal analysis. **Abdulrahman I. Almansour:** Formal analysis. **A. Sakthisabarimoorthi:** Formal analysis. **J. Kalyana Sundar:** Formal analysis. **S.A. Martin Britto Dhas:** Supervision, Investigation, Writing – review & editing.

Declaration of Competing Interest

The authors declare no competing financial interests.

Acknowledgment

The authors thank Sacred Heart College for Don Bosco Research Grant (SHC/DB Grant/2021/01) and NSF of China (42072055). The project was also supported by Researchers Supporting Project number (RSP2023R142), King Saud University, Riyadh, Saudi Arabia.

References

[1] T. Sakuntala, A.K. Arora, N.V. Chandra Shekar, P.C. Sahu, Orientational disorder: a mechanism of amorphization at high pressure, Europhys. Lett. 44 (1998) 728–733.
[2] B.S. Yilbas, A.F.M. Arif, S.Z. Shuja, Investigation into laser shock processing, J. Mater. Eng. Perform. 13 (2004) 47–54.
[3] Kaixiang Liu, Li dong Dai, Heping Li, Haiying Hu, Linfei Yang, Chang Pu, Meiling Hong, Evidences for phase transition and metallization in β−In2S3 at high pressure, Chem. Phys. 524 (2019) 63–69.
[4] H. Yin, Q. Sun, Temperature variation in NiTi shape memory alloy during cyclic phase transition, J. Mater. Eng. Perform. 21 (2012) 2505–2508.
[5] F. El-kabbany, G. Said, Y. Baur, S. Tah;, Infrared investigation of the phase transition in K_2SO_4, Phys. Status Solidi A 67 (1981) 339.
[6] S.B. Anooz, R. Bertram, D. Klimm;, The solid state phase transformation of potassium sulfate, Solid State Commun. 141 (2007) 497–501.
[7] Byoung Koo Choi, David J. Lockwood, Peculiarities of the structural phase transitions in Na_2SO_4(V): a Raman scattering study, J. Phys. Condens. Matter 17 (2005) 6095–6108.
[8] Raul Kabert, Leif Nilssont, Niels Hessel Andersent, Arnold Lundent, John Thomas, A single-crystal neutron diffraction study of the structure of the high-temperature rotor phase of lithium sulphate, J. Phys. Condens. Matter 4 (1992) 1925–1933.
[9] V. Lernos, C.S. Sergio, High-pressure phase transitions in Li_2SO_4, Phys. Rev. B 41 (1990) 593–596.
[10] Encarnacion Ruiz-Agudo, J.Daniel Martin-Ramos, Carlos Rodriguez-Navarro, Mechanism and kinetics of dehydration of epsomite crystals formed in the presence of organic additives, J. Phys. Chem. B 111 (2007) 41–52.

[11] S. El-Houte, M. El-Sayed Ali, O. Toft Sorensen, Dehydration of $CuSO_4{\cdot}5H_2O$ studied by the conventional and advanced thermal analysis studies, Thermochim. Acta 138 (1989) 107–114.

[12] Shuiquan Lan, Herbert Zondag, Anton van Steenhoven, Camilo Rindt, An experimentally validated numerical model of interface advance of the lithium sulfate monohydrate dehydration reaction, J. Therm. Anal. Calorim. 124 (2016) 1109–1118.

[13] A. Sivakumar, S. Reena Devi, S. Sahaya Jude Dhas, R. Mohan Kumar, K. Kamala Bharathi, S.A. Martin BrittoDhas;, Switchable phase transformation (orthorhombic−hexagonal) of potassium sulfate single crystal at ambient temperature by shock waves, Cryst. Growth Des. 20 (2020) 7111–7119.

[14] A. Sivakumar, S. Sahaya Jude Dhas, P. Sivaprakash, Abdulrahman I. Almansour, Raju Suresh Kumar, S.Arumugam NatarajanArumugam, S.A. Martin BrittoDhas, The switchable phase transition of sodium sulfate crystals activated by shock waves, New J. Chem. 45 (2021) 16529.

[15] A. Sivakumar, S. Sahaya Jude Dhas, Shubhadip Chakraborty, Raju Suresh Kumar, Abdulrahman I. Almansour, Natarajan Arumugam, S.A. Martin Britto Dhas, Dynamic shock wave induced amorphous to crystalline switchable phase transition of lithium sulfate, J. Phy. Chem. C 126 (2022) 3194–3201.

[16] A. Sivakumar, P. Shailaja, S. Sahaya Jude Dhas, P. Sivaprakash, Abdulrahman I. Almansour, Raju Suresh Kumar, Natarajan Arumugam, S. Arumugam, Shubhadip Chakraborty, S.A. Martin Britto Dhas, Dynamic shock wave-induced switchable phase transition of magnesium sulfate heptahydrate, Cryst. Growth Des. 21 (2021) 5050–5057.

[17] A. Sivakumar, S. Sahaya Jude Dhas, Abdulrahman I. Almansour, Raju Suresh Kumar, Natarajan Arumugam, S.A. Martin Britto Dhas, Switchable phase transition between crystalline and amorphous states of $CuSO_4{\cdot}5H_2O$ by dynamic shock waves, CrystEngComm 23 (2021) 7044.

[18] A. Sivakumar, S. Sahaya Jude Dhas, P. Sivaprakash, Raju Suresh Kumar, Abdulrahman I. Almansour, Karthikeyan Perumal, S. Arumugam, S.A. Martin Britto Dhas, Shock wave induced reversible phase transition from crystalline to semi-crystalline states of lithium sulfate monohydrate, J. Solid State Chem 307 (2022), 122859.

[19] A. Sivakumar, S. Sahaya Jude Dhas, Abdulrahman I. Almansour, Raju Suresh Kumar, Natarajan Arumugam, Karthikeyan Perumal, S.A. Martin Britto Dhas, A comparative analysis of structural properties on single and poly-crystalline potassium sulfate crystals at shock wave loaded conditions, Solid State Commun. 340 (2021), 114508.

[20] A. Sivakumar, S. Sahaya Jude Dhas, Raju Suresh Kumar, Abdulrahman I. Almansour, Magesh Murugesan, S.A. Martin Britto Dhas, High shock resistance of poly- crystalline sodium sulfate crystals at dynamic shocked conditions, Phys. Status Solidi B 259 (2022) 2100540.

[21] A. Sivakumar, S. Sahaya Jude Dhas, J. Elberin Mary Theras, M. Jose, P. Sivaprakash, S. Arumugam, S.A. Martin Britto Dhas, Spectroscopic and diffraction studies of polycrystalline copper sulfate pentahydrate at shocked conditions, Solid State. Sci 121 (2021), 106751.

[22] A. Silambarasan, P. Rajesh, R. Bhatt, I. Bhaumik, K.K. Maurya, A.K. Karnal, P. Ramasamy, P.K. Gupta, Investigation on the structural, linear/nonlinear optical and electrical characteristics of Cd- and Mn-doped polar lithium sulfate monohydrate crystals, New J. Chem. 41 (2017) 12259–12267.

[23] K. Boopathi, P. Rajesh, P. Ramasamy, Growth of negative solubility lithium sulfate monohydrate crystal by slow evaporation and Sankaranarayanan–Ramasamy method, J. Cryst. Growth 345 (2012) 1–6.

[24] A. Silambarasan, E. Nageswara Rao, S. Venugopal Rao, P. Rajesh, P. Ramasamy, Bulk growth, crystalline perfection and optical characteristics of inversely soluble lithium sulfate monohydrate single crystals grown by conventional solvent evaporation and modified Sankaranarayanan-Ramasamy method, CrystEngComm 18 (2016) 2072–2080.

[25] M.M. Naik, F.A. Mir, F. Ullah, P.A. Ahmad, B.A. Ghayas, Brief study on structural, optical, and photovoltaic properties of lithium sulfate monohydrate single crystals, J. Mater. Sci. Mater. Electron 31 (2020) 11855–11861.

[26] F.A. Najar, G.B. Vakil, B. Want, Structural, optical and dielectric studies of lithium sulphate monohydrate single crystals, Mater. Sci. Poland 35 (2017) 18–31.

[27] M. Karppinen, R. Liminga, Å. Kvick, S.C. Abrahams, Diffraction derived spontaneous polarization in lithium sulfate monohydrate at 80 and 298 K, J. Chem. Phys. 88 (1988) 351.

[28] Andrew K. Galwey, Nobuyoshi Koga, Haruhiko Tanaka, A kinetic and microscopic investigation of the thermal dehydration of lithium sulphate monohydrate, J. Chem. Soc. Faraday Trans. 86 (1990) 531–537.

[29] Shuiquan Lan, Herbert Zondag, Anton van Steenhoven, Camilo Rindt, Kinetics study of the dehydration reaction of lithium sulfate monohydrate crystals using microscopy and modeling, Thermochim. Acta 621 (2015) 44–55.

[30] N.A. Simakova, N.Z. Lyakhov, N.A. Rudina, Thermal dehydration of lithium sulfate monohydrate. the reaction reversibility and the solid product morphology, Thermochim. Acta 256 (1995) 381–389.

[31] A.J.D. Pim, B. Steffen, P. Leo, S. Frank, S. Michael, C.G.A. Olaf, Water transport in $MgSO_4$ $7H_2O$ during dehydration in view of thermal storage, J. Phys. Chem. C 119 (2015) 28711–28720.

[32] A. Sivakumar, S. Sahaya Jude Dhas, S. Balachandar, S.A. Martin Britto Dhas, Impact of shock waves on molecular and structural response of potassium dihydrogen phosphate crystal, J. Elect. Mater. 48 (2019) 7868–7873.

[33] A. Sivakumar, S. Sahaya Jude Dhas, S.A. Martin Britto Dhas, Impact of shock waves on vibrational and structural properties of glycine phosphite, Solid State Sci. 110 (2020), 106452.

[34] M. Hafok, R. Pippan, Comparison of single crystalline and polycrystalline behavior under high pressure torsion, Mater. Sci. Forum 550 (2007) 277–282.

[35] Laurent Mezeix, David J. Green, Comparison of the mechanical properties of single crystal and polycrystalline yttrium aluminum garnet, Int. J. Appl. Ceram. Technol. 3 (2006) 166–176.

[36] Guijun Yang, Soo Jin Park, Deformation of single crystals, polycrystalline materials, and thin films: a review, Material 12 (2019) 2003.

[37] R.P. Canterford, F. Ninio;, Raman study of polar phonons in lithium sulphate monohydrate, J. Phys. C Solid State Phys. 8 (1975) 1750–1762.

[38] Enzo Cazzanelli, Roger Frech;, Temperature dependent Raman spectra of monoclinic and cubic Li_2SO_4, J. Chem. Phys. 81 (1984) 4729.

[39] Enzo Cazzanelli, Roger Frech;, Raman spectra of Li_2SO_4 and Li_2SO_4, J. Chem. Phys. 79 (1983) 2615.

[40] Xinyu Zhang, Lidong Dai, Haiying Hu, Chuang Li, Pressure-induced reverse structural transition of calcite at temperatures up to 873 K and pressures up to 19.7 GPa, Minerals 13 (2023) 188.

[41] Xiao Tan, Kai Wang, Tingting Yan, Xiaodong Li, Jing Liu, Ke Yang, Bingbing Liu, Guangtian Zou, Bo Zou, Discovery of high-pressure polymorphs for a typical polymorphic system: oxalyl dihydrazide, J. Phys. Chem. C 119 (2015) 10178–11018.

[42] Yuejian Wang, Joseph E. Panzik, Boris Kiefer, Kanani K.M. Lee;, Crystal structure of graphite under room-temperature compression and decompression, Sci. Rep. 2 (2012) 520.

[43] A. Sivakumar, A. Saranraj, S. Sahaya Jude Dhas, M. Jose, K. Kamala Bharathi, S. A. Martin Britto Dhas, Modification of optical properties of ammonium dihydrogen phosphate crystal by employing shock waves, Opt. Eng. 58 (2019), 107101.

[44] A. Sivakumar, A. Saranraj, S. Sahaya Jude Dhas, K. Showrilu, S.A. Martin Britto Dhas, Phase stability analysis of shocked ammonium dihydrogen phosphate by X-ray and Raman scattering studies, Z. Kristallogr. 236 (2021) 1–10.

[45] M.S. Dileep, H.M. Suresh Kumar, Sindhu Tilak, Mechanical, electrical, linear and nonlinear optical behavior of gamma irradiated thiourea doped lithium sulfate single crystals, Can. J. Phys. 99 (2021) 1–14.

[46] C.M. Julien, A. Ait-Salah, A. Mauger, F. Gendron, Magnetic properties of lithium intercalation compound, Ionics 12 (2006) 21–32 (Kiel).

[47] W. Senanon, P. Phaiboon, N. Chanlek, Y.P. Arporn, S. Pinitsoontorn, S. Maensirid, J. Khajonrit, P. Kidkhunthod, Effect of Mn on lithium-sulphate-borated based glass as energy storage applications, J. Non Cryst. Solid 552 (2021), 120445.

[48] J. Elberin Mary Theras, D. Kalaivani, J. Arul Martin Mani, D. Jayaraman, V. Joseph, Synthesis, structural and optical properties, ferromagnetic behaviour, cytotoxicity and NLO activity of lithium sulphate doped L-threonine, Optic. Laser Technol. 83 (2016) 49–54.

[49] V. Mowlika, A. Sivakumar, S.A. Martin Britto Dhas, C.S. Naveen, A.R. Phani, R. Robert, Shock waveinduced switchable magnetic phase transition behaviour of $ZnFe_2O_4$ ferrite nanoparticles, J. Nanostruct. Chem. 10 (2020) 203–209.

[50] V. Mowlika, C.S. Naveen, A.R. Phani, A. Sivakumar, S.A. Martin Britto Dhas, R. Robert, Shock wave induced magnetic phase transition in cobalt ferrite nanoparticles, Mater. Chem. Phys. 275 (2022), 125300.

[51] Dennis Zywitzki, Dereje H. Taffa, Laura Lamkowski, Manuela Winter, Detlef Rogalla, Michael Wark, Anjana Devi, Tuning coordination geometry of nickel ketoiminates and its influence on thermal characteristics for chemical vapor deposition of nanostructured NiO electrocatalysts, Inorg. Chem. 59 (2020) 10059–10070.

[52] Mohammad Sajjad Hossain, Md.Badiul Alamy, Mohammad Shahjahan, Most. Hosney Ara Begum, Md.Moazzem Hossain, Suravi Islam, Nazia Khatun, Mukul Hossainz, Mohammad Saiful Alamy, Md. Al-Mamun, Synthesis, structural investigation, dielectric and magnetic properties of Zn^{2+} doped cobalt ferrite by the sol–gel technique, J. Adv. Dielectr. 8 (2018), 1850030.

[53] Zhi Su, William L. Shaw, Yu Run Miao, Sizhu You, Dana D. Dlott, Kenneth S. Suslick, Shock wave chemistry in a metal−organic framework, J. Am. Chem. Soc. 139 (2017) 4619–4622.

[54] Xuan Zhou, Yu Run Miao, William L. Shaw, Kenneth S. Suslick, Dana D. Dlott, Shock wave energy absorption in metal−organic framework, J. Am. Chem. Soc. 141 (2019) 2220–2223.